

# Holographic p-wave Superconductors in Quasi-topological Gravity

Xiao-Mei Kuang<sup>1,\*</sup>, Wei-Jia Li<sup>2,†</sup> and Yi Ling<sup>1‡</sup>

<sup>1</sup>*Center for Relativistic Astrophysics and High Energy Physics,*

*Department of Physics, Nanchang University, 330031, China*

<sup>2</sup>*Department of Physics, Beijing Normal University, Beijing 100875, China*

## Abstract

We construct a holographic p-wave superconductor model in the framework of quasi-topological gravity in the probe limit. The relation between the critical temperature and the coupling parameters of higher curvature terms is investigated. The numerical results for conductivity are presented as well. It turns out that our data fits the Drude model very well in the low frequency limit, and the values of DC conductivity as well as the relaxation time are obtained numerically.

PACS numbers: 04.70.Bw, 11.25.Hf, 74.20..z

arXiv:1106.0784v2 [hep-th] 4 Apr 2012

---

\*Electronic address: xmeikuang@gmail.com

†Electronic address: li831415@163.com

‡Electronic address: yling@ncu.edu.cn

## I. INTRODUCTION

Recently the gauge/gravity duality[1–3] has been widely applied to the study of condensed matter physics. In particular, some critical phenomena in strongly coupled systems can be described by the dynamics of geometry as well as matter fields in a semi-classical region (For recent reviews we refer to [4–7]). One remarkable example is building holographic superconductor models based on the Abelian Higgs mechanism, through which an asymptotical anti-de Sitter black hole can break the  $U(1)$  gauge symmetry spontaneously [8]. In these models, when the effective mass of a scalar field in the bulk is below the Breitenlohner-Freedman bound [9], a hairy solution to the scalar field can be obtained, characterized by its condensation around the horizon of the black hole. According to AdS/CFT correspondence, the creation of charged condensation strongly implies that a second order phase transition could occur in the dual CFT[10–13]. Furthermore, this sort of holographic superconductors contain more interesting features[14–25]. For instance, the energy gap is much larger than the predictions of the conventional BCS theory but quite similar to the high- $T_c$  superconductors as found in experiments[26].

In addition to various holographic s-wave superconductor models with scalar fields, one can also construct p-wave superconductor models with vector fields, implemented by introducing a  $SU(2)$  Yang-Mills gauge field[27–32]. Correspondingly, the dual CFT has a global  $SU(2)$  symmetry and hence a conserved current  $J_\mu^i$ . In the AdS black hole background, it is found that the  $U(1)_3$  gauge symmetry (a subgroup of  $SU(2)$ ) is possibly spontaneously broken such that the value of  $\langle J_x^1 \rangle$  is not vanishing. This corresponds to a phase transition between a non-superconducting state at high temperature and a superconducting state below the critical temperature. However, different from the s-wave model, here the order parameter is a current and the conductivity is anisotropic since the condensation of vector field breaks the rotational symmetry as well. As a result the conductivity has two independent components. One perpendicular to the direction of the condensation behaves like that in s-wave superconductors, while the other parallel to it performs a much different behavior. In particular, this component agrees well with the Drude model in the low frequency limit.

Recently a gravity theory with nontrivial curvature-cubed terms in five-dimensional spacetime, usually called quasi-topological gravity, has been proposed in [33–37]. This theory can be viewed as a generalization of Gauss-Bonnet gravity. Besides the GB term in the

action, it also involves in higher-derivative corrections, thereby corresponding to CFTs with more couplings between operators as discussed in [38, 39]. As a matter of fact, the holographic study of the quasi-topological gravity has been carried out in many references[39–43] and its dual CFTs display much richer structures and novel features. Specially, in this theory two central charges relating to the conformal anomaly can be unequal, which brings in a non-zero but much lower bound of the ratio of shear viscosity to density entropy and hence violation of the Kovtun-Son-Starinets (KSS) bound[39]. In this paper, we intend to continue our previous investigation on holographic s-wave superconductors in [41], and construct a holographic p-wave model in the framework of quasi-topological gravity. We are specially concerned with the anisotropic behavior of the gauge fields and intend to compare our results with other p-wave models in Einstein’s and Gauss-Bonnet gravity. We will also discuss the charge transport using a linear response theory, with a special interest in its behavior in the low frequency limit.

We organize our paper as follows. In Sec.II, we present the holographic setup for a p-wave superconductor in quasi-topological gravity, then study the superconducting phase transition in the probe limit, focusing on the variation of the critical temperature with the coupling parameters. Sec.III contributes to the numerical evaluation of the anisotropic conductivity. Based on the data obtained we mainly discuss the following two issues. One is on the change of the ratio of the frequency gap to the critical temperature with the frequency, and the other is on the low frequency behavior of the conductivity. Discussions and conclusions are given in Sec.IV.

## II. QUASI-TOPOLOGICAL HOLOGRAPHIC P-WAVE SUPERCONDUCTORS

We start with the five-dimensional quasi-topological gravity with an SU(2) Yang-Mills gauge field. The bulk action is given as

$$S_{bulk} = \int d^5x \sqrt{-g} \left[ \frac{1}{16\pi G_5} \left( R + \frac{12}{L^2} + \frac{\alpha L^2}{2} \mathcal{X}_4 + \frac{7\beta L^4}{8} \mathcal{Z}_5 \right) - \frac{1}{4g_{YM}^2} (F_{\mu\nu}^i F^{i\mu\nu}) \right], \quad (1)$$

where  $G_5$  is the Newton constant in five-dimensional theory, and  $\alpha$ ,  $\beta$  and  $g_{YM}$  are Gauss-Bonnet coupling parameter, curvature-cubed interaction parameter and Yang-Mills coupling parameter, respectively.  $F_{\mu\nu}^i$  is the field strength of Yang-Mills gauge field with SU(2) gauge

symmetry and  $i$  is the internal index. Here  $\mathcal{X}_4$  is the Gauss-Bonnet term

$$\mathcal{X}_4 = R_{\mu\nu\rho\sigma}R^{\mu\nu\rho\sigma} - 4R_{\mu\nu}R^{\mu\nu} + R^2, \quad (2)$$

and  $\mathcal{Z}_5$  is a curvature-cubed term with the form

$$\begin{aligned} \mathcal{Z}_5 = & R_{\mu\nu}{}^{\rho\sigma}R_{\rho\sigma}{}^{\alpha\beta}R_{\alpha\beta}{}^{\mu\nu} + \frac{1}{14}(21R_{\mu\nu\rho\sigma}R^{\mu\nu\rho\sigma}R - 120R_{\mu\nu\rho\sigma}R^{\mu\nu\rho}{}_{\alpha}R^{\sigma\alpha} \\ & + 144R_{\mu\nu\rho\sigma}R^{\mu\rho}R^{\nu\sigma} + 128R_{\mu}{}^{\nu}R_{\nu}{}^{\rho}R_{\rho}{}^{\mu} - 108R_{\mu}{}^{\nu}R_{\nu}{}^{\mu}R + 11R^3). \end{aligned} \quad (3)$$

It is worthy to point out that in contrast to higher order terms in Lovelock gravity[44], the cubed terms above are not just topological but have contributions to equations of motion for bulk fields. Through this paper we will only take account of the probe limit of the theory. Namely, we will neglect the back reaction of the Yang-Mills field on the background metric in the large  $N_c$  limit, where  $N_c$  is the number of degrees of freedom per point in the dual free field theory <sup>1</sup>.

In this limit stable AdS black hole solutions in five-dimensional spacetime have been found in [33] and they can be described as

$$ds^2 = \frac{r^2}{L^2}(-N(r)^2f(r)dt^2 + dx^2 + dy^2 + dw^2) + \frac{L^2}{r^2f(r)}dr^2, \quad (4)$$

where  $f(r)$  has three different solutions for different regions in parameter space

$$f_1(r) = u + v - \frac{\alpha}{3\beta}, \quad (5)$$

$$f_2(r) = -\frac{1}{2}(u + v) + i\frac{\sqrt{3}}{2}(u - v) - \frac{\alpha}{3\beta}, \quad (6)$$

$$f_3(r) = -\frac{1}{2}(u + v) - i\frac{\sqrt{3}}{2}(u - v) - \frac{\alpha}{3\beta}, \quad (7)$$

with

$$\begin{aligned} u &= (q + \sqrt{q^2 - p^3})^{1/3}, & v &= (q - \sqrt{q^2 - p^3})^{1/3}, \\ p &= \frac{3\beta + \alpha^2}{9\beta^2}, & q &= -\frac{2\alpha^3 + 9\alpha\beta + 27\beta^2(1 - \frac{r_H^4}{r^4})}{54\beta^3}. \end{aligned} \quad (8)$$

---

<sup>1</sup> The large  $N_c$  limit implies  $G_5 \sim N_c^{-2} \rightarrow 0$ , leading to a decoupling between the matter field with a finite  $g_{YM}$  and the gravity in the action  $S_{bulk}$ .

$L$  is the AdS radius and  $N(r) = N = 1/\sqrt{f(r)|_{r \rightarrow \infty}}$  is the lapse function<sup>2</sup>. Now it is straightforward to obtain the Hawking temperature of these black holes, which is

$$T = \frac{N}{4\pi} f'(r)|_{r=r_H} = \frac{Nr_H}{\pi L^2}. \quad (9)$$

It will also be viewed as the temperature of the dual CFT on the boundary.

Now we turn to construct the holographic p-wave superconductors. Firstly we need to solve the Yang-Mills equations in a fixed black hole background. Following the strategy presented in [8], we take the ansatz as follows

$$A_a = A_\mu^i \tau^i (dx^\mu)_a = \tilde{\phi}(r) \tau^3 (dt)_a + \tilde{\psi}(r) \tau^1 (dx)_a, \quad (10)$$

where  $\tau^i = \sigma^i/2i$  ( $i=1,2,3$ ) with commutation relations  $[\tau^i, \tau^j] = i\epsilon^{ijk} \tau^k$  are SU(2) generators. In (10) the nonvanishing  $\tilde{\psi}(r)$  breaks the  $U(1)_3$  gauge symmetry generated by  $\tau^3$ . We may interpret it as the p-wave superconducting phase transition from the side of CFT on the boundary, since in the dual field theory the global  $U(1)_3$  symmetry is broken and superconducting charges can be created from the new vacuum which corresponds to the formation of the Cooper pairs. For convenience, we absorb the gauge couplings into the rescaling of the gauge fields

$$\phi = g_{YM} L^2 \tilde{\phi}, \quad \psi = g_{YM} L^2 \tilde{\psi}. \quad (11)$$

Moreover, we redefine the coordinate  $z = \frac{r_H}{r} = \frac{1}{r}$  such that the position of the horizon is fixed at  $z = 1$ , while the boundary is  $z \rightarrow 0$ . Then with the ansatz in Eq.(10) the equations for Yang-Mills field reduce to the following form

$$\phi'' - \frac{\phi'}{z} - \frac{L^2 \psi^2}{z^2 g} \phi = 0, \quad (12)$$

$$\psi'' + \left(\frac{g'}{g} + \frac{1}{z}\right) \psi' + \frac{\phi^2}{N^2 g^2 z^4} \psi = 0, \quad (13)$$

where  $g = \frac{r^2 f(r)}{L^2}$  and the prime denotes a derivative with respect to  $z$ . Before solving these two equations we give the boundary conditions near the horizon and near the AdS boundary as follows:

---

<sup>2</sup> In order to get a normalized velocity of light on the boundary, the lapse function  $N$  usually should not be set to unit. This gauge is different from that in [32] and some discrepancy of our results for GB gravity with those in [32] can be ascribed to this different gauge. Moreover, the argument that  $N(r)$  is a constant can be seen in [33].

◆ The regularity condition at the horizon ( $z = 1$ ) requires the gauge fields should be expanded as

$$\begin{aligned}\psi &= \psi_H^{(0)} + \psi_H^{(2)}(1-z)^2 + \dots \\ \phi &= \phi_H^{(1)}(1-z) + \dots\end{aligned}\tag{14}$$

◆ Near the AdS boundary ( $z \rightarrow 0$ ), the asymptotical behavior of fields are like

$$\begin{aligned}\psi &= \psi^{(0)} + \psi^{(2)}z^2 + \dots \\ \phi &= \mu + \rho z^2 + \dots\end{aligned}\tag{15}$$

In AdS/CFT dictionary,  $\mu$  is the chemical potential on the boundary while  $\rho_t = 2\rho$  and  $\rho_n = \phi_H^{(1)}$  are understood as the total charge density and the charge density in the normal state, respectively. So the p-wave superconducting charge density is  $\rho_s = \rho_t - \rho_n$ . A nonzero  $\psi^{(0)}$  and nonzero  $\psi^{(2)}$  correspond to a source and the expectation value of vacuum for the current operator  $J_x^1$  that is dual to the gauge field  $A_x^1 = \psi$  respectively, so we have

$$\langle J_x^1 \rangle = \psi^{(2)}.\tag{16}$$

For normalizable modes, the expectation value of vacuum can be obtained by setting  $\psi^{(0)} = 0$ .

Before doing the numerical analysis, we present some remarks on the allowed range of the values of the coupling parameters  $\alpha$  and  $\beta$ . First of all, to obtain the stable black hole solutions without ghost modes or naked singularity, one finds that the allowed parameter range is constrained in the region as illustrated in the left plot of FIG.1[33]. On the other hand, to ensure the positivity of central charges, energy flux and a well-defined causality for the dual CFT,  $\alpha$  and  $\beta$  are further severely confined into a small region as dictated in the right plot of FIG.1, which has originally been presented in [39]. Thus in our paper we will investigate the holographic superconductivity with parameter values restricted in this small region. However, in this region the coupling constant  $\beta$  is severely restricted in a narrow interval, roughly from  $\beta = -0.001$  to  $\beta = 0.001$ . Graphically when one changes the value of  $\beta$  in this region, the plotting is probably not sensitive enough to illustrate the changes of the physical quantities with different values of the coupling constants. Thus we take two actions in our plotting. One is to enlarge a local region in figures to demonstrate the shifting tendency of the curves with the values of coupling parameters. Secondly, we also take some

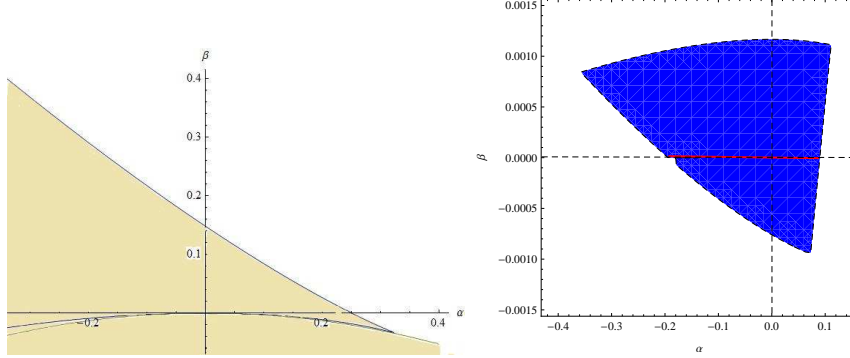


FIG. 1: The allowed range of the values of coupling parameters  $\alpha$  and  $\beta$ : In the left plot, the yellow region is for the stable solution and the different regions divided by the color lines correspond to different stable black hole solutions given by (5) – (7) (see [33] for details); In the right plot, the blue region is the valid parameter range restricted by consistency of the dual CFT, and the red line corresponds to  $\beta = 0$ , i.e., the constraint of  $\alpha$  in Gauss-Bonnet gravity.

value for  $\beta$  from the region in the left plot of FIG.1 for comparison, for instance  $\beta = 0.1$ . In the probe limit we are allowed to do this since the back reaction of the perturbations is not taken into account and we may still obtain the stable phase in dual field theory, but it is warned that the curves obtained for these values are potentially unstable for a system when the back reaction of the perturbations is considered, thus should not be trusted seriously.

Now to explore the p-wave superconducting phase, we need find nonzero solutions for  $\psi$  by numerical analysis. In our program, we set  $L = 1$  and find the numerical solutions to the differential EOMS from the horizon to the AdS boundary, namely, from  $z \rightarrow 1$  to  $z \rightarrow 0$ . In Figure 2, we illustrate the condensation of  $J_x^1$  as the function of the temperature with different values of coupling parameters  $\alpha$  and  $\beta$ . Note that different from the case of s-wave superconductor, here we plot the dimensionless quantity  $\frac{\sqrt[3]{J_x^1}}{T_c}$  with respect to  $\frac{T}{T_c}$  since the conformal dimension of  $J_x^1$  is 3 rather than 1 for  $T_c$ . FIG.2 indicates that the order parameter has the behavior  $\langle J_x^1 \rangle \propto (1 - T/T_c)^{1/2}$  near the critical temperature, and the value of  $\frac{\sqrt[3]{J_x^1}}{T_c}$  increases with both the Gauss-Bonnet coupling parameter  $\alpha$  and the curvature-cubed coupling parameter  $\beta$ , which is similar to the phenomenon obtained in the s-wave superconductor in quasi-topological gravity[41], as well as the p-wave superconductors in Gauss-Bonnet gravity [32].

In figure 3, we plot  $\rho_s/\rho_t$  v.s.  $\frac{T}{\sqrt[3]{\rho}}$  by changing either of the coupling parameters  $\alpha$  and  $\beta$ . The critical temperatures for different coupling parameters can be read off from the

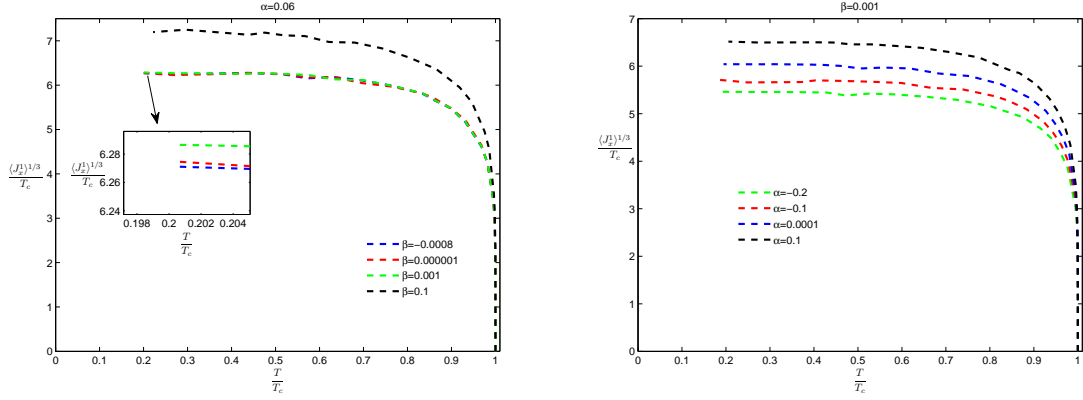


FIG. 2: The condensate as a function of the temperature with different values of coupling parameters. In the left figure, the Gauss-Bonnet parameter  $\alpha$  is fixed at 0.06.  $\beta$  is fixed at 0.001 in the right figure. In both cases the condensation tends to increase with the coupling parameters.

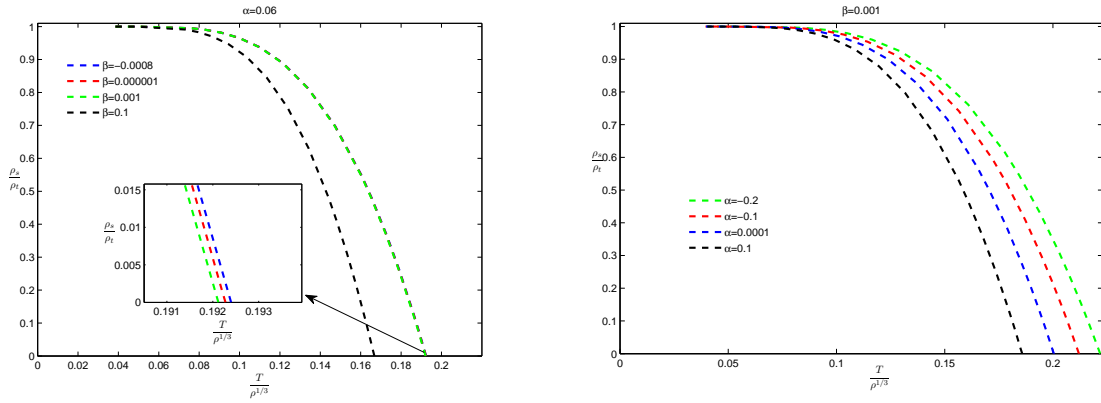


FIG. 3: The ratio of the superconducting charge density to the total charge density v.s. the temperature with different values of coupling parameters.

intersects with the horizontal axis and their values are listed in TABLE I. We can see that the critical temperature decrease as either  $\alpha$  or  $\beta$  increases, implying that with the increase of the curvature-cubed term or the Gauss-Bonnet term the occurrence of condensation should become harder. This tendency is the same as those in the previous papers[32, 41]. For explicitness we demonstrate the dependence of the critical temperature on either of the coupling parameter in FIG.4. Moreover, in [39] we know the conformal field dual to the quasi-topological gravity is characterized by central charges,  $c$  and  $a$ , and flux parameters,  $t_2$  and  $t_4$ . Explicitly, these parameters can be related to the coupling parameters in the



| $\alpha$ | $\beta$  | $T_c$              |
|----------|----------|--------------------|
| 0.06     | -0.0008  | $0.1924\rho^{1/3}$ |
| 0.06     | 0.000001 | $0.1923\rho^{1/3}$ |
| 0.06     | 0.001    | $0.1921\rho^{1/3}$ |
| 0.06     | 0.1      | $0.1667\rho^{1/3}$ |
| -0.2     | 0.001    | $0.2218\rho^{1/3}$ |
| -0.1     | 0.001    | $0.2120\rho^{1/3}$ |
| 0.0001   | 0.001    | $0.2004\rho^{1/3}$ |
| 0.1      | 0.001    | $0.1858\rho^{1/3}$ |

TABLE I: The change of the critical temperature with the coupling parameter  $\alpha$  and  $\beta$ . The critical temperatures corresponding to the parameter values in FIG.3 are listed in two tables respectively.

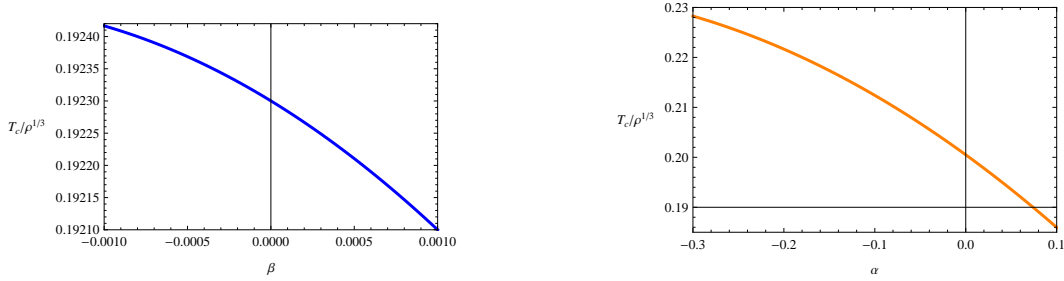


FIG. 4: The relations between  $T_c$  and the coupling parameters  $\alpha$  and  $\beta$ , respectively. In the left figure the line is for  $\alpha = 0.06$ , while in the right figure the line is for  $\beta = 0.001$ .

bulk as follows

$$\delta = \frac{c - a}{c} = \frac{4f_\infty(\alpha - 3\beta f_\infty)}{1 - 2\alpha f_\infty - 3\beta f_\infty^2}, \quad (17)$$

$$t_2 = \frac{24f_\infty(\alpha - 87f_\infty\beta)}{1 - 2\alpha f_\infty - 3\beta f_\infty^2} \quad (18)$$

$$t_4 = \frac{3780f_\infty^2\beta}{1 - 2\alpha f_\infty - 3\beta f_\infty^2}, \quad (19)$$

where  $f_\infty$  satisfies  $1 - f_\infty + \alpha f_\infty^2 + \beta f_\infty^3 = 0$ . Among these parameters any two of them is enough to describe the correlations in the dual CFT. For example, we can calculate  $\delta$  and  $t_4$  as the free parameters and fit how  $T_c$  changes with the changing of  $\delta$  and  $t_4$  respectively.

However, as discussed in [41], a clear rule from the CFT side is still missing, thus we will not show the fitting plot of the critical temperature versus  $\delta$  or  $t_4$  in our current paper.

In the next section, we turn to investigate the conductivity and find its new characters comparing with the s-wave superconductors.

### III. CONDUCTIVITY

In this section, we will study the charge transport and linear response of the boundary system. In the linear response theory, a central quantity is the retarded Green function. According to the AdS/CFT dictionary, if we want to know the retarded Green function of the  $U(1)$  current, we just need to study the propagation of the linear perturbation of the gauge field in the bulk in the probe limit. So, in the following, we are interested in the linear response of the  $\tau^3$  component of the Yang-Mills gauge field. As discussed in [8], we can consider an alternating current(AC) on the boundary by introducing a time-dependent perturbation for the gauge field

$$A \rightarrow A + \delta A, \quad (20)$$

where

$$\delta A = e^{-i\omega t} \left[ \left( a_t^1(r)\tau^1 + a_t^2(r)\tau^2 \right) dt + a_x^3(r)\tau^3 dx + a_y^3(r)\tau^3 dy \right]. \quad (21)$$

Though the condensation of  $\psi$  breaks the rotational  $SO(3)$  symmetry associated with  $x$  direction, the system still has an  $SO(2)$  symmetry in  $y-w$  plane. Hereafter, we neglect the perturbation along  $w$ -axis and only consider the electrical conductivity  $\sigma_{xx}$  and  $\sigma_{yy}$ .

#### 1. $\sigma_{yy}$ component

Substituting the ansatz in (21) into the Yang-Mills equations, we obtain the equation of motion for  $a_y^3$

$$a_y^{3''} + \left( \frac{g'}{g} + \frac{1}{z} \right) a_y^{3'} + \left( \frac{\omega^2}{N^2 g^2 z^4} - \frac{L^2 \psi^2}{z^2 g} \right) a_y^3 = 0, \quad (22)$$

where the prime is relative to  $z = 1/r$ . In general, different modes of the perturbations are mixed, however, from the equation above we notice that  $a_y^3$  is actually decoupled from other components. In addition, the equation is similar to that for s-wave superconductors [32, 41],

so we can obtain the conductivity  $\sigma_{yy}$  in a parallel way. Specifically, we choose the ingoing wave condition for  $a_y^3$  near the horizon, then we have

$$a_y^3 = (1 - z)^{\frac{-i\omega}{4N}} [1 + a_y^{3(1)}(1 - z) + a_y^{3(2)}(1 - z)^2 + \dots]. \quad (23)$$

Moreover, the behavior of  $a_y^3$  in the asymptotical AdS boundary ( $z \rightarrow 0$ ) is

$$a_y^3 = a_y^{3(0)} + a_y^{3(2)} z^2 + \frac{a_y^{3(0)} \omega^2 N^4}{2} (\log \Lambda/z) z^2, \quad (24)$$

where  $a_y^{3(0)}$ ,  $a_y^{3(2)}$  and  $\Lambda$  are integration constants. The last term in (24) will lead to a divergence when one calculates the Green function, however, such a logarithmic divergence can be canceled with a boundary counterterm in the renormalization procedure[45]. Thanks to the standard AdS/CFT dictionary, the conductivity can be expressed through the retarded Green function as follows[46]

$$\sigma(\omega) = \frac{1}{i\omega} G^R(\omega) \Big|_{\mathbf{k}=\mathbf{0}} = -\frac{1}{i\omega} \lim_{r \rightarrow \infty} N g(r) r a_y^3 a_y^{3'}, \quad (25)$$

Thus we find the conductivity  $\sigma_{yy}$  is<sup>3</sup>

$$\sigma_{yy} = = \frac{2a_y^{3(2)}}{i\omega N^3 a_y^{3(0)}} - i\omega N \ln N + \frac{iN\omega}{2}. \quad (26)$$

Given the boundary conditions (23) and (24), we numerically solve equation (22) to obtain  $a_y^{3(0)}$  and  $a_y^{3(2)}$ . As a result, the dependent relation between  $\sigma_{yy}$  and  $\omega$  for different coupling parameters  $\beta$  and  $\alpha$  are shown in FIG.5 and FIG.6, respectively. From these two figures, it is clear that when the frequency  $\omega$  is large enough, the real part of  $\sigma_{yy}$  always increases while the imaginary part becomes linear due to the dominant term  $\omega N \ln N + \frac{N\omega}{2}$ . In addition, from the imaginary part of conductivity one finds that the ratio  $\omega_g/T_c$  increases with either  $\alpha$  or  $\beta$ . This behavior is much similar to that of  $\sigma$  in the s-wave case[41], while it is interesting to note that for p-wave superconductor the values of the real part of conductivity increase with the coupling parameters. Since this quantity corresponds to the imaginary part of the Green function which characterizes the dissipation of the charge transport, this phenomenon is analogous to what happens in holographic hydrodynamics as described in figure 2 in [39].

---

<sup>3</sup> As pointed out in [47], the term  $-i\omega N \ln N$  should not be neglected. Though we take a different gauge here, the asymptotic analysis near the boundary is similar and a direct calculation shows that the result is the same.

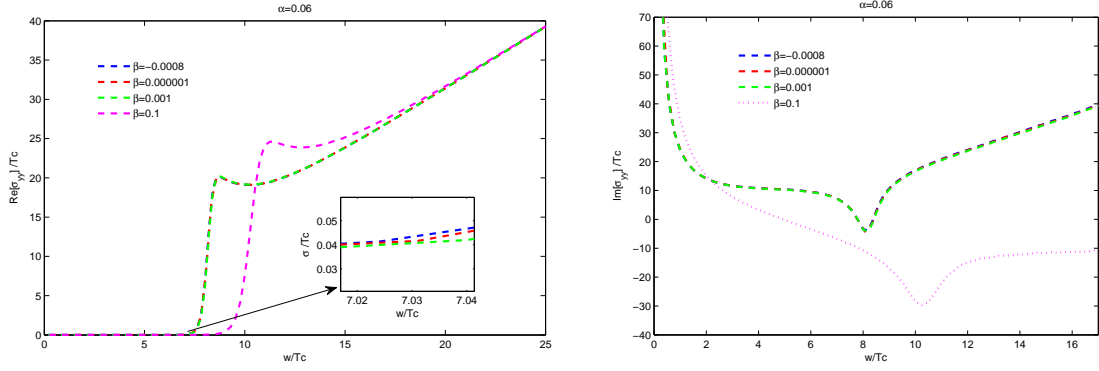


FIG. 5: The conductivity  $\sigma_{yy}$  for the p-wave superconductors with a fixed Gauss-Bonnet parameter  $\alpha = 0.06$ . The left figure is for the real part of  $\sigma_{yy}$  while the right one is for the imaginary part of  $\sigma_{yy}$ .

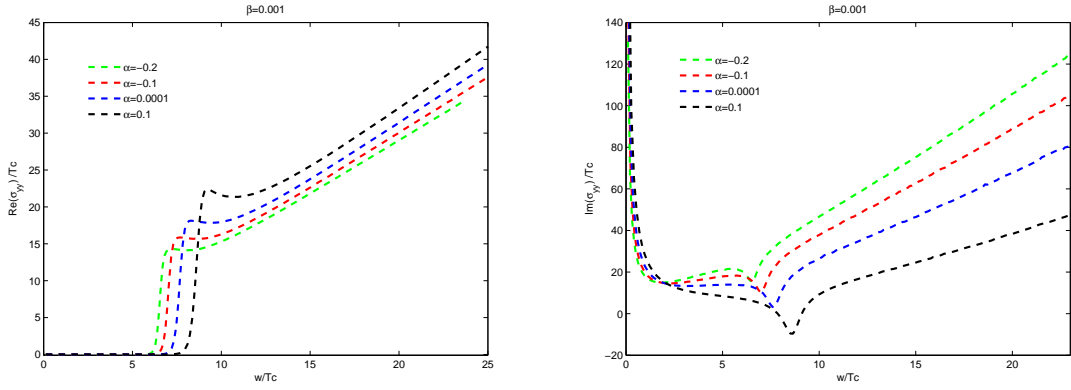


FIG. 6: The conductivity  $\sigma_{yy}$  for the p-wave superconductors with a fixed the curvature-cubed parameter  $\beta = 0.001$ . Similarly, the left figure is for the real part of  $\sigma_{yy}$  while the right one is for the imaginary part of  $\sigma_{yy}$ .

## 2. $\sigma_{xx}$ component

Now we intend to study the component  $\sigma_{xx}$ , which can be obtained by solving the equation of motion for  $a_x^3$  in the bulk. In contrast to  $a_y^3$ , since the component  $a_x^3$  couples with the fields  $a_t^1$  and  $a_t^2$  in the linearized Yang-Mills equations, besides three second-order coupling

equations of motion

$$\begin{aligned}
a_x^{3''} + \left(\frac{1}{z} + \frac{g'}{g}\right)a_x^{3'} + \frac{\omega^2}{g^2 N^2 z^4} a_x^3 - \frac{i\omega a_t^2 + a_t^1 \phi}{g^2 N^2 z^4} \psi &= 0, \\
a_t^{1''} - \frac{1}{z} a_t^{1'} + \frac{L^2 a_x^3 \phi \psi}{z^2 g} &= 0, \\
a_t^{2''} - \frac{1}{z} a_t^{2'} - \frac{L^2 \psi^2}{z^2 g} a_t^2 - \frac{iL^2 \omega a_x^3 \psi}{z^2 g} &= 0,
\end{aligned} \tag{27}$$

we need to solve another two first-order equations together

$$\begin{aligned}
-i\omega a_t^{1'} - \phi a_t^{2'} + a_t^2 \phi' &= 0, \\
\phi a_t^{1'} - i\omega a_t^{2'} + L^2 N^2 g \psi a_x^{3'} z^2 - a_t^1 \phi' - L^2 a_x^3 N^2 g \psi' z^2 &= 0.
\end{aligned} \tag{28}$$

Again using the ingoing wave condition near the horizon, we have the following asymptotical behavior of  $a_y^3$ ,  $a_t^1$  and  $a_t^2$ :

► Near the horizon ( $z \rightarrow 1$ )

$$a_x^3 = (1-z)^{\frac{-i\omega}{4N}} [1 + A_x^{3(1)}(1-z) + A_x^{3(2)}(1-z)^2 + \dots], \tag{29}$$

$$a_t^1 = (1-z)^{\frac{-i\omega}{4N}} [A_t^{1(2)}(1-z)^2 + A_t^{1(3)}(1-z)^3 + \dots], \tag{30}$$

$$a_t^2 = (1-z)^{\frac{-i\omega}{4N}} [A_t^{2(1)}(1-z) + A_t^{2(2)}(1-z)^2 + \dots]. \tag{31}$$

► Near the boundary of the AdS bulk ( $z \rightarrow 0$ )

$$a_x^3 = a_x^{3(0)} + a_x^{3(2)} z^2 + \frac{a_x^{3(0)} \omega^2 N^4 \log(\Lambda/z) z^2}{2} + \dots, \tag{32}$$

$$a_t^1 = a_t^{1(0)} + a_t^{1(2)} z^2 + \dots, \tag{33}$$

$$a_t^2 = a_t^{2(0)} + a_t^{2(2)} z^2 + \dots. \tag{34}$$

All the coefficients can be determined numerically. However, these quantities are gauge dependent since we have not done any gauge fixing to these components. As discussed in [8], in order to obtain the conductivity  $\sigma_{xx}$  we need define a gauge invariant quantity as follows

$$\hat{a}_x^3 = a_x^3 + \frac{i\omega L^2 a_t^2 + \phi a_t^1}{\phi^2 - \omega^2 L^4} \psi. \tag{35}$$

Then we have the asymptotical behavior of  $\hat{a}_x^3$  near the AdS boundary

$$\begin{aligned}
\hat{a}_x^3 &= a_x^{3(0)} + a_x^{3(2)} z^2 + \frac{a_x^{3(0)} \omega^2 N^4 \log(\Lambda/z) z^2}{2} + \frac{i\omega L^2 a_t^{2(0)} + \mu a_t^{1(0)}}{\mu^2 - \omega^2 L^4} \psi^{(2)} z^2 \\
&= a_x^{3(0)} + \hat{a}_x^{3(2)} z^2 + \frac{a_x^{3(0)} \omega^2 N^4 \log(\Lambda/z) z^2}{2},
\end{aligned} \tag{36}$$

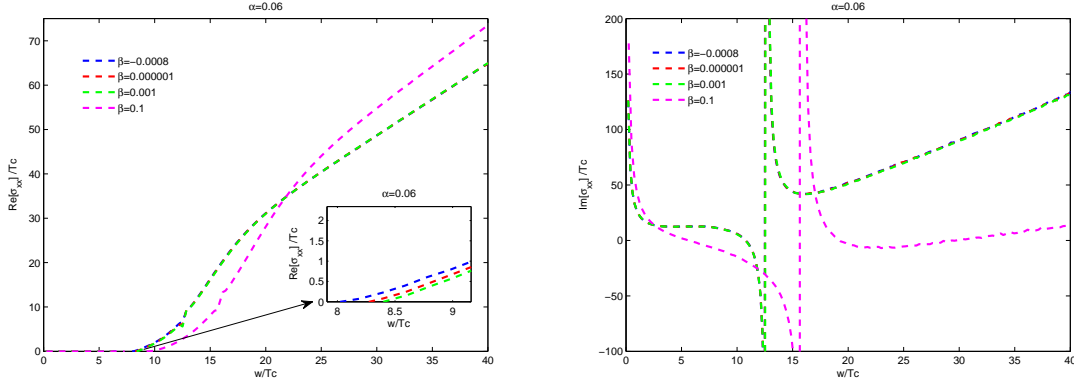


FIG. 7: The conductivity  $\sigma_{xx}$  for the p-wave superconductors with a fixed  $\alpha$ . The left figure is for the real part of  $\sigma_{xx}$  while the right one is for the imaginary part of  $\sigma_{xx}$ .

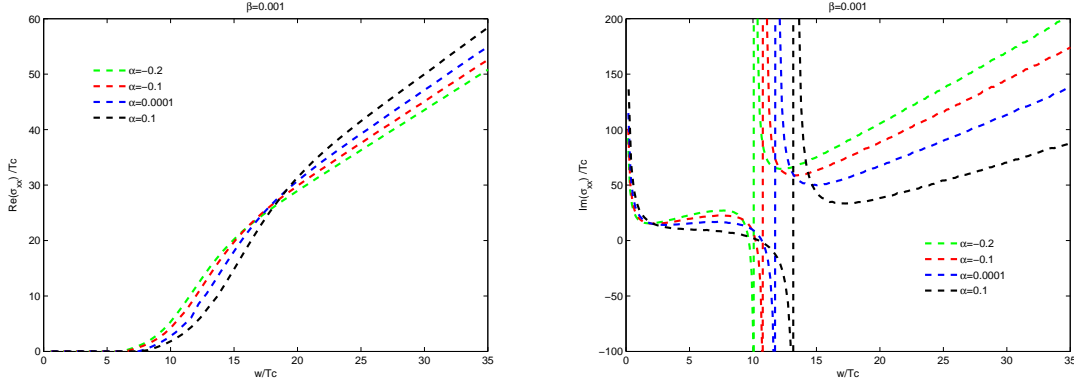


FIG. 8: The conductivity  $\sigma_{xx}$  for the p-wave superconductors with a fixed curvature-cubed parameter  $\beta = 0.001$ . Similarly, the left figure is for the real part of  $\sigma_{xx}$  while the right one is for the imaginary part of  $\sigma_{xx}$ .

where we have defined

$$\hat{a}_x^{3(2)} = a_x^{3(2)} + \frac{i\omega L^2 a_t^{2(0)} + \mu a_t^{1(0)}}{\mu^2 - \omega^2 L^4} \psi^{(2)}. \quad (37)$$

As a result, the conductivity  $\sigma_{xx}$  has the form

$$\sigma_{xx} = \frac{1}{i\omega} G^R(\omega) \Big|_{k=0} = -\frac{2i\hat{a}_x^{3(2)}}{a_x^{3(0)}\omega N^3} - i\omega N \ln N + \frac{1}{2}i\omega N. \quad (38)$$

In order to understand the behavior of  $\sigma_{xx}$ , we simultaneously solve the equation groups (12), (13), (27) as well as (28). The numerical results of  $\sigma_{xx}$  are shown in FIG.7 and FIG.8.

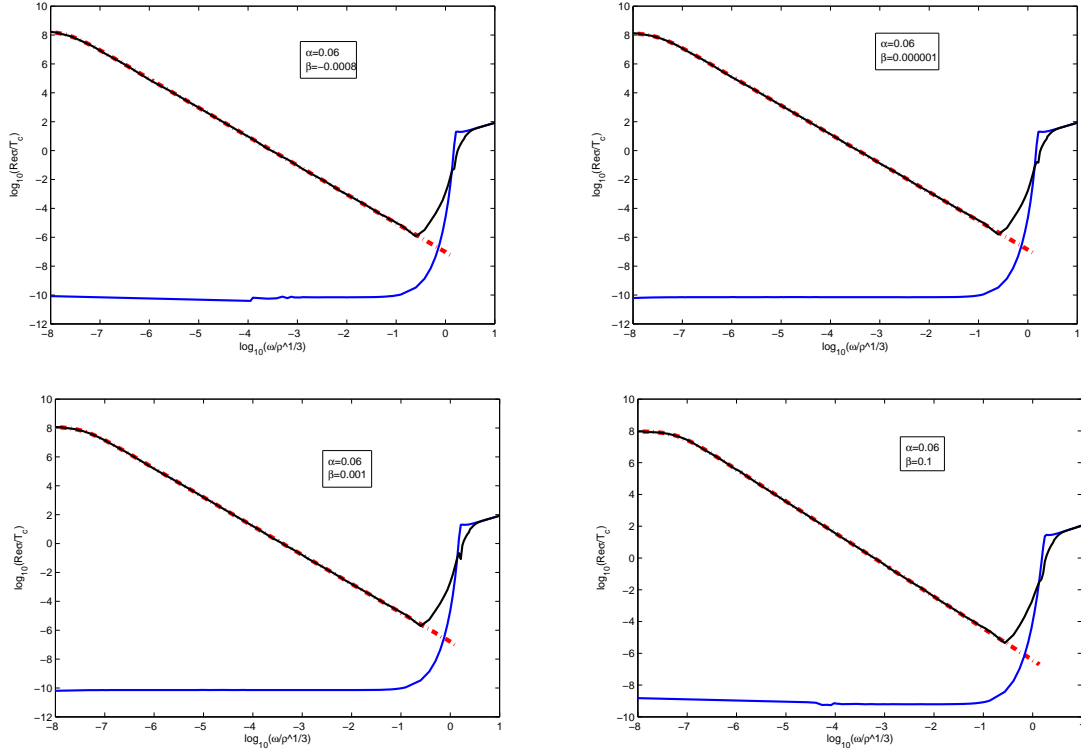


FIG. 9: The relations between  $\log_{10}[Re(\sigma/T_c)]$  and  $\log_{10}[\omega/\rho^{(1/3)}]$  for fixed  $\alpha = 0.06$ . The blue and black lines are for  $\sigma_{yy}$  and  $\sigma_{xx}$  respectively, while the red ones are the fitting lines of  $\sigma_{xx}$  when  $\omega$  is low enough.

| $\alpha$ | $\beta$  | $\sigma_0/T$         | $\tau T$             |
|----------|----------|----------------------|----------------------|
| 0.06     | -0.0008  | $1.0213 \times 10^9$ | $1.8304 \times 10^6$ |
| 0.06     | 0.000001 | $7.5091 \times 10^8$ | $1.3064 \times 10^6$ |
| 0.06     | 0.001    | $6.4602 \times 10^8$ | $1.1072 \times 10^6$ |
| 0.06     | 0.1      | $5.6827 \times 10^8$ | $6.38 \times 10^5$   |
| -0.2     | 0.001    | $3.735 \times 10^9$  | $8.804 \times 10^6$  |
| -0.1     | 0.001    | $2.5534 \times 10^9$ | $5.588 \times 10^6$  |
| 0.0001   | 0.001    | $1.5959 \times 10^9$ | $3.2288 \times 10^6$ |
| 0.1      | 0.001    | $8.7646 \times 10^8$ | $1.6036 \times 10^6$ |

TABLE II: The evaluation of  $\sigma_0$  and  $\tau$  and their dependence on the values of coupling parameters.

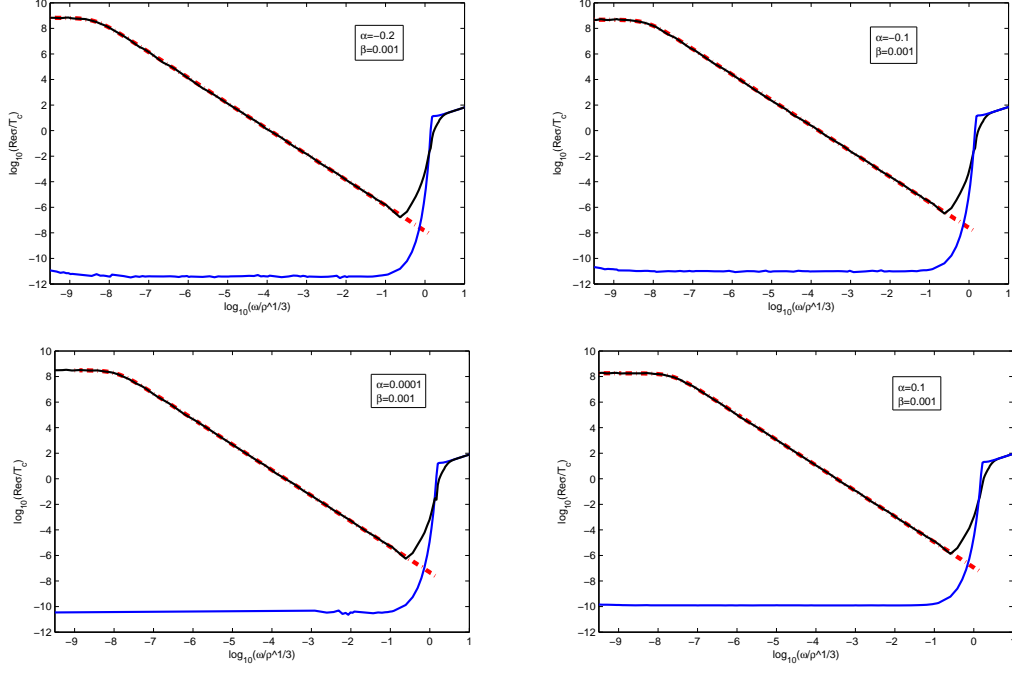


FIG. 10: The relations between  $\log_{10}[Re(\sigma/T_c)]$  and  $\log_{10}[\omega/\rho^{(1/3)}]$  for fixed  $\beta = 0.001$ . The blue and black lines are for  $\sigma_{yy}$  and  $\sigma_{xx}$  respectively, while the red ones are the fitting lines of  $\sigma_{xx}$  when  $\omega$  is low enough.

In these two figures, we find that the point of phase transition will also change when we choose different couplings, but the behavior of the component  $\sigma_{xx}$  is very different from that of component  $\sigma_{yy}$ . Comparing with  $\sigma_{yy}$ , the real part of  $\sigma_{xx}$  ascends much more slowly. In the high frequency limit, the imaginary part has a suppression effect with the increase of the coupling parameters. On the other hand, in the low frequency limit,  $\sigma_{xx}$  behaves quite like that in Drude model, and this analogy was firstly observed by Gubser in [8]. Drude model is conventionally used to describe the classical electron system, in which the real part of the conductivity is featured by the relation

$$Re(\sigma) = \frac{\sigma_0}{1 + \omega^2\tau^2}, \quad (39)$$

where  $\sigma_0 = ne^2\tau/m$  is the DC conductivity,  $n$ ,  $e$ ,  $m$ ,  $\tau$  are the electron density, charge, mass and the relaxation time respectively. Based on the Drude relation, we can fit our numerical results to evaluate  $\sigma_0$  and  $\tau$  in FIG. 9 and FIG .10. All the fittings are done under the condition that the condensation is stable, namely, the value of  $T/\rho^{1/3}$  is small enough. We



show the fitting results of  $\sigma_0$  and  $\tau$  and their dependence on couplings parameters  $\alpha$  and  $\beta$  in TABLE II. From the table, we find that both of  $\sigma_0$  and  $\tau$  depend on the coupling parameters.

#### IV. DISCUSSIONS AND CONCLUSIONS

In this paper we have constructed a p-wave holographic superconductor model in quasi-topological gravity in the probe limit. Firstly, we find that the superconducting condensation becomes harder with the increase of the GB coupling and curvature-cubed coupling. This is very similar to the case of the s-wave model. Secondly, both anisotropic conductivities  $\sigma_{xx}$  and  $\sigma_{yy}$  are studied. The numerical results indicate that the behavior of  $\sigma_{yy}$  at the low temperature is quite similar to that in the s-wave model. More precisely, with the increase of coupling parameters  $\alpha$  or  $\beta$  the ratio  $\omega_g/T_c \approx 8$  becomes unstable and increases as well. However, the conductivity  $\sigma_{xx}$  behaves differently. Its real part grows more slowly with the frequency, while its imaginary part contains a spike. For both components, the imaginary part is always suppressed by the increasing of couplings in the large frequency limit. While in the low frequency limit, our data of  $\sigma_{xx}$  fits the Drude model very well, but the values of DC conductivity as well as the relaxation time depend on the coupling parameters.

It is worth pointing that due to the presence of higher curvature corrections in quasi-topological gravity, besides the ghost modes and naked singularity one should also be cautious of other potential instabilities, such as the dynamical instability as discussed in [48] for Lovelock gravity and the plasma instability as discussed in [39, 49]. Those potential instabilities may further restrict the valid values of the coupling parameters [39, 48, 49]. We leave this open issue for further investigation in future.

In the end of this paper we remark that it should be very worthy to investigate p-wave superconductors when the back reactions are taken into account in our model. It is expected that both the condensation and the charge transport would be corrected by the effects of back reactions [13, 30, 32, 43, 50]. Moreover, inspired by recent progress on the holographic non-fermion liquid and strange metals [51–56], it might be possible to explore fermion system with a finite charge density in the framework of the quasi-topological gravity. In these systems, the fermion part near the horizon has a loop contribution to the total two point correlator of the current, however, such an  $O(N^0)$  contribution dominates the dissipation

of the transport[57]. Since in quasi-topological gravity the bulk of spacetime may exhibit a richer structure of geometry due to the higher order couplings, we propose that the dual CFTs would show different behavior at low energy limit. This is expected to be done in future.

### Acknowledgments

We are grateful to Jian-Pin Wu, Hai-Qing Zhang and Hongbao Zhang for reply and useful discussions. X. M. Kuang and Y. Ling is partly supported by NSFC(Nos.10663001,10875057), JiangXi SF(Nos. 0612036, 0612038), Fok Ying Tung Education Foundation(No. 111008), the key project of Chinese Ministry of Education(No.208072) and Jiangxi young scientists(JingGang Star) program. W. J. Li is partly supported by NSFC (No. 10975016). We also acknowledge the support by the Program for Innovative Research Team of Nanchang University.

- 
- [1] J. M. Maldacena, The large N limit of superconformal field theories and supergravity, *Adv. Theor. Math. Phys.* 2, 231 (1998) [*Int. J. Theor. Phys.* 38, 1113 (1999)] [hep-th/9711200].
  - [2] E. Witten, Anti-de Sitter space and holography, *Adv. Theor. Math. Phys.* 2 (1998) 253-291, [hep-th/9802150].
  - [3] O. Aharony, S. S. Gubser, J. M. Maldacena, H. Ooguri, and Y. Oz, Large N field theories, string theory and gravity, *Phys. Rept.* 323 (2000) 183-386, [hep-th/9905111].
  - [4] S. A. Hartnoll, Lectures on holographic methods for condensed matter physics, *Class. Quant. Grav.* 26, 224002 (2009) [arXiv:0903.3246].
  - [5] J. McGreevy, Holographic duality with a view toward many-body physics, arXiv:0909.0518.
  - [6] S. Sachdev, Condensed matter and AdS/CFT, arXiv:1002.2947v1 [hep-th].
  - [7] Gary T. Horowitz, Surprising Connections Between General Relativity and Condensed Matter, *Class.Quant.Grav.*28:114008,2011, arXiv:1010.2784[gr-qc].
  - [8] S. S. Gubser, Breaking an Abelian gauge symmetry near a black hole horizon, *Phys. Rev. D* 78, 065034 (2008) ,arXiv:0801.2977.
  - [9] P. Breitenlohner and D. Z. Freedman, Positive Energy in anti-De Sitter Backgrounds and

- Gauged Extended Supergravity, Phys. Lett. B115 (1982) 197.
- [10] S. A. Hartnoll, C. P. Herzog and G. T. Horowitz, Building a Holographic superconductor, Phys. Rev. Lett. 101:031601, 2008, arXiv:0803.3295.
  - [11] S. A. Hartnoll, C. P. Herzog and G. T. Horowitz, Holographic Superconductors, JHEP12(2008)015, arXiv:0810.1563v1 [hep-th].
  - [12] C. P. Herzog, Lectures on Holographic Superfluidity and Superconductivity, J. Phys. A: Math. Theor. 42 343001, arXiv:0904.1975v2 [hep-th].
  - [13] Gary T. Horowitz, Introduction to Holographic Superconductors, arXiv:1002.1722v2 [hep-th]
  - [14] Q. Pan, Bin Wang, E. Papantonopoulos, J. Oliveria and A. B. Pavan, Holographic Superconductors with various condensates in Einstein-Gauss-Bonnet gravity, Phys.Rev.D 81, (2010) 106007, arXiv:0912.2475[hep-th].
  - [15] Xi He, Bin Wang, Rong-Gen Cai, Chi-Yong Lin, Signature of the black hole phase transition in quasinormal modes, Phys. Lett. B 688 230, arXiv:1002.2679 [hep-th].
  - [16] Xian-Hui Ge, Bin Wang, Shao-Feng Wu, Guo-Hong Yang, Analytical study on holographic superconductors in external magnetic field, J. High Energy Phys. JHEP08(2010)108, arXiv:1002.4901 [hep-th].
  - [17] Q. Pan and B. Wang, General holographic superconductor models with Gauss-Bonnet corrections, Phys.Lett. B693 (2010) 159 arXiv:1005.4743 [hep-th].
  - [18] Xin Gao, Hongbao Zhang, Refractive index in holographic superconductors, JHEP 1008:075,2010 arXiv:1008.0720v1 [hep-th].
  - [19] Jian-Pin Wu, Yue Cao, Xiao-Mei Kuang, Wei-Jia Li, The 3+1 holographic superconductor with Weyl corrections, Phys.Lett.B697:153-158,2011, arXiv:1010.1929v3 [hep-th].
  - [20] J. Jing, L.Wang, Q. Pan and S. Chen, Holographic Superconductors in Gauss-Bonnet gravity with Born-Infeld electrodynamics, Phys. Rev. D 83 (2011) 066010 arXiv:1012.0644 [gr-qc].
  - [21] S. Chen, Q. Pan and J. Jing, Holographic superconductor models in the non-minimal derivative coupling theory, arXiv:1012.3820[hep-th].
  - [22] Sugumi Kanno, A Note on Gauss-Bonnet Holographic Superconductors, Class.Quant.Grav.28:127001,2011, arXiv:1103.5022v2 [hep-th]
  - [23] Y. Peng, Q. Pan and B. Wang, Various types of phase transitions in the AdS soliton background, Phys. Lett. B 699 383C7, arXiv:1104.2478[hep-th].
  - [24] Qiyuan Pan, Jiliang Jing, Bin Wang, Analytical investigation of the phase transition between

- holographic insulator and superconductor in Gauss-Bonnet gravity, *J. High Energy Phys.* JHEP11(2011)088, arXiv:1105.6153 [hep-th].
- [25] Gregory R, Kanno S and Soda J 2009 Holographic superconductors with higher curvature corrections arXiv:0907.3203v3 [hep-th]
- [26] K. K. Gomes, A. N. Pasupathy, A. Pushp, S. Ono, Y. Ando and A. Yazdani, "Visualizing pair formation on the atomic scale in the high-Tc superconductor  $Bi_2Sr_2CaCu_2O_{8+\delta}$ ," *Nature* 447, 569 (2007).
- [27] S. S. Gubser, Colorful horizons with charge in anti-de Sitter space, *Phys. Rev. Lett.*101:191601,2008, arXiv:0803.3483v1 [hep-th].
- [28] S. S. Gubser and S. S. Pufu, The gravity dual of a p-wave superconductor, *JHEP* 0811:033,2008, arXiv:0805.2960v2 [hep-th].
- [29] R. G. Cai, Z. Y. Nie and H. Q. Zhang, Holographic p-wave superconductors from Gauss-Bonnet gravity, *Phys. Rev. D* 82, 066007 (2010), arXiv:1007.3321 [hep-th]
- [30] M. Ammon, J. Erdmenger, V. Grass, P. Kerner and A. O'Bannon, On Holographic p-wave Superfluids with Back-reaction, *Phys.Lett.B*686:192-198,2010, arXiv:0912.3515v2 [hep-th]; M. Ammon, J. Erdmenger, M.Kaminski and A. O'Bannon, Fermionic Operator Mixing in Holographic p-wave Superfluids, *JHEP* 1005:053,2010, arXiv:1003.1134v2 [hep-th].
- [31] H. B. Zeng, Z. Y. Fan and H. S. Zong, *Phys.Rev.D*81:106001,2010, arXiv:0912.4928v4 [hep-th].
- [32] R. G. Cai, Z. Y. Nie and H. Q. Zhang, Holographic Phase Transitions of P-wave Superconductors in Gauss-Bonnet Gravity with Back-reaction, *Phys.Rev.D*83:066013,2011, arXiv:1012.5559v2 [hep-th].
- [33] R. C. Myers and B. Robinson, Black Holes in Quasi-topological Gravity, *JHEP* 08(2010)067, arXiv:1003.5357v2.
- [34] J. Oliva and S. Ray, A new cubic theory of gravity in five dimensions: Black hole, Birkhoffs theorem and C-function, *Class.Quant.Grav.*27:225002,2010, arXiv:1003.4773 [gr-qc].
- [35] J. Oliva and S. Ray, A Classification of Six Derivative Lagrangians of Gravity and Static Spherically Symmetric Solutions, *Phys.Rev.D*82:124030,2010, arXiv:1004.0737 [gr-qc].
- [36] A. Sinha, On the new massive gravity and AdS/CFT, *JHEP* 1006061 (2010), arXiv:1003.0683 [hep-th].
- [37] A. Sinha, On higher derivative gravity, c-theorems and cosmology, *Class. Quant. Grav.*28:085002,2011, arXiv:1008.4315[hep-th].

- [38] D. M. Hofman, Higher Derivative Gravity, Causality and Positivity of Energy in a UV complete QFT, Nucl. Phys. B 823, 174 (2009) [arXiv:0907.1625 [hep-th]].
- [39] R.C. Myers, M. F. Paulos and A. Sinha, Holographic studies of quasi-topological gravity, JHEP 08(2010)035, arXiv:1004.2055v2 [hep-th].
- [40] A. J. Amsel, D. Gorboson, The Weak Gravity Conjecture and the Viscosity Bound with Six-Derivative Corrections, JHEP 1011:033,2010, arXiv:1005.4718[hep-th].
- [41] X. M. Kang, W. J. Li and Y. Ling, Holographic Superconductors in Quasi-topological Gravity, JHEP 1012:069,2010, arXiv:1008.4066 [hep-th].
- [42] K. B. Fadafan, Heavy quarks in the quasi-topological gravity, arXiv:1102.2289v1 [hep-th].
- [43] M. Siani, Holographic Superconductors and Higher Curvature Corrections, JHEP 1012:035,2010, arXiv:1010.0700v1 [hep-th].
- [44] D. Lovelock, J. Math. Phys. 12, 498 (1971). D. J. Gross and J. H. Sloan, Nucl. Phys. B 291, 41 (1987). R. R. Metsaev and A. A. Tseytlin, Nucl. Phys. B 293, 385 (1987).
- [45] M. T. Robinson, arXiv:hep-th/0002125.
- [46] D. T. Son and A. O. Starinets, Minkowski-space correlators in AdS/CFT correspondence: Recipe and applications, JHEP 0209, 042 (2002), arXiv:hep-th/0205051.
- [47] L. Barclay, R. Gregory, S. Kanno and P. Sutcliffe, Gauss-Bonnet Holographic Superconductors, JHEP 1012:029,2010, arXiv:1009.1991 [hep-th].
- [48] T. Takahashi, J. Soda, [arXiv:1108.5041 [hep-th]].
- [49] X. O. Camanho, J. D. Edelstein, M. F. Paulos, JHEP 1105, 127 (2011). [arXiv:1010.1682 [hep-th]].
- [50] Xian Hui Ge, Analytical calculation on critical magnetic field in holographic superconductors with backreaction, arXiv:1105.4333 [hep-th].
- [51] S. S. Lee, Phys. Rev. D 79 (2009) 086006 [arXiv:0809.3402 [hep-th]].
- [52] H. Liu, J. McGreevy and D. Vegh, Non-Fermi liquids from holography, Phys.Rev.D83:065029,2011, arXiv:0903.2477v3 [hep-th]; T. Faulkner, N. Iqbal, H. Liu, J. McGreevy and David Vegh, From black holes to strange metals, arXiv:1003.1728v1 [hep-th].
- [53] S. A. Hartnoll, J. Polchinski, E. Silverstein and D. Tong, Towards strange metallic holography, JHEP 1004:120,2010, arXiv:0912.1061v2 [hep-th]; T. Faulkner and Joseph Polchinski, Semi-Holographic Fermi Liquids, arXiv:1001.5049v2 [hep-th]; K. Jensen, S. Kachru, A. Karch, J.

- Polchinski and E. Silverstein, Towards a holographic marginal Fermi liquid, arXiv:1105.1772v1 [hep-th].
- [54] M. Cubrovic, J. Zaanen and K. Schalm, Science 325 (2009) 439 [arXiv:0904.1993 [hep-th]].
- [55] S. Sachdev, Strange metals and the AdS/CFT correspondence, J.Stat.Mech.1011:P11022,2010, arXiv:1010.0682v3 [cond-mat.str-el].
- [56] J. P. Wu, Holographic fermions in charged Gauss-Bonnet black hole, JHEP 1107:106,2011 arXiv:1103.3982v2 [hep-th].
- [57] T. Faulkner, N. Iqbal, H. Liu, J. McGreevy and D. Vegh, Strange Metal Transport Realized by Gauge/Gravity Duality, Science 329, 1043 (2010).